1 Seasonal and Diurnal Variations in Moisture, Heat and CO₂ Fluxes over a

2 **Typical Steppe Prairie in Inner Mongolia, China**

3

Z. Gao¹, D. H. Lenschow², Z. He¹, M. Zhou^{1,3}, L. Wang¹, Y. Wang⁴, J. He⁴, J.

Shi^4

- 1. State Key Laboratory of Atmospheric Boundary Layer Physics and Atmospheric Chemistry, Institute of Atmospheric Physics, CAS, Beijing, China
- 2. National Center for Atmospheric Research (NCAR), Boulder CO, USA
- 4 3. Key Laboratory for Polar Science, Polar Research Institute of China, Shanghai, China
 - 4. Xilinhaote Meteorological Station, Inner Mongolia, China

5

Abstract

In order to examine energy partitioning and CO_2 exchange over a steppe prairie in 6 7 Inner Mongolia, China, fluxes of moisture, heat and CO_2 in the surface layer from June 2007 through June 2008 were calculated using the eddy covariance method. The study site 8 9 was homogenous and approximately 1500 m \times 1500 m in size. Seasonal and diurnal 10 variations in radiation components, energy components and CO_2 fluxes are examined. Results show that all four radiation components changed seasonally, resulting in a seasonal 11 12 variation in net radiation. The radiation components also changed diurnally. Winter surface albedo was higher than summer surface albedo because during winter the snow-covered 13 surface increased the surface albedo. The seasonal variations in both sensible heat and CO_2 14 fluxes were stronger than those of latent heat and soil heat fluxes. This implies that both 15 sensible heat and CO_2 fluxes may be more significant climate signals than latent heat and 16 soil fluxes. Sensible heat flux was the main consumer of available energy for the entire 17 experimental period. The energy imbalance problem was encountered and the causes are 18 19 analyzed.

- 1
- 2 Keywords: turbulent fluxes, eddy covariance, steppe prairie, Inner Mongolia
- 3
- 4

5 **1. Introduction**

6

7 The relatively recent increase in atmospheric carbon dioxide (hereinafter, referred to as CO_2) concentration has profound implications for the planet's climate (see, for example, 8 the IPCC report) as well as on photosynthesis and the structure and function of plant 9 10 Vegetation therefore plays a crucial role in the global carbon balance communities, (Woodward et al., 1998; Mielnick et al., 2001). The energy budget balance over land 11 12 surfaces is the most important of all the ecological processes related to carbon sequestration in terrestrial ecosystems (Baldocchi et al., 1997; Dugas et al., 1999; Hao et al., 2007). 13 Surface fluxes of momentum, heat and moisture determine to a large extent the steady state 14 of the atmosphere (Beljaars and Holtslag, 1991). Climate simulations are especially 15 sensitive to the seasonal and diurnal variations in surface partitioning of available energy 16 17 into sensible and latent heat fluxes (e.g., Rowntree, 1991; Dickinson et al., 1991).

In order to evaluate the long-term energy balance and evapotranspiration, a number of experimental studies have been carried out on various terrestrial surfaces such as forest, grasslands and paddy fields throughout the world during the past decade (e.g., Baldocchi and Vogel, 1997; Toda *et al.*, 2002; Gao, *et al.*, 2003; Bi *et al.*, 2006; Hao *et al.*, 2007). Previous work has reported on measurements of the seasonal and/or diurnal variations of heat, water vapor and CO₂ exchanges over different land surfaces in a variety of ecosystems
ranging from the tropics to the northern high latitudes (e.g., Hartog, *et al.*, 1994; Delire, *et al.*, 1995; Betts, *et al.*, 1995; Campbell, *et al.*, 2001; Vourlitis *et al.*, 2001; Merquiol, *et al.*,
2002; Xue *et al.*, 2004; Barros, *et al.*, 2005; Steven, *et al.*, 2005; Bi *et al.*, 2006; ; Hao et al.,
2007).

6 Grasslands are approximately 32% of the Earth's natural vegetation (Adams et al., 1990) 7 and grassland ecosystems undergo considerable annual fluctuations in gross primary production (Frank and Dugas, 2001); grassland ecosystems also significantly and 8 asymmetrically nonlinearly respond to climate change and pertinent biomass dynamics 9 (Baldocchi et al., 2001; Wever et al., 2002). Prior researchers mainly paid attention to 10 savanna areas and the Central Great Plains of the U.S. (Dugas et al., 1999; Frank and Dugas, 11 12 2001; Sims and Bradford, 2001; Suyker and Verma, 2001; Novick et al., 2004). In contrast, there are few works focused on measurements of the seasonal and/or diurnal variations of 13 heat, water vapor and CO₂ exchanges in the great steppes of Asia (Li et al., 2006; Hao et al., 14 15 2007) because much of the data obtained so far is still insufficient. The Eurasian Steppe, within which Inner Mongolia lies, is the largest grassland region 16 in the world. This part of the Steppe lies in a semi-arid temperate continental climate regime 17 (Hao et al., 2007). Climate change will result in a wintertime warming trend and severe 18 springtime drought in this region (Chen et al., 2003). Therefore it is important to understand 19 the seasonal and diurnal variations of water vapor and energy within this grassland 20 ecosystem. Unfortunately, there is currently little detailed information on this in the 21 22 literature.

23

24 We conducted a micrometeorological experiment over a natural steppe prairie in Inner

Mongolia from June 2007 to improve the current understanding of energy partitioning and CO_2 exchange over a typical steppe prairie in Inner Mongolia and to find which surface energy components show the strongest climate signals. The main objective of the present work is therefore to quantify the seasonal and diurnal variations in energy and CO_2 exchanges over the above mentioned surface using eddy covariance techniques.

6 2. Materials and Methods

7 2.1 Site

Measurements have been collected at a grassland site (44°08'31"N, 116°18'45"E, 1160.8 8 9 m above sea level) in the typical steppe prairie in Inner Mongolia since June 1, 2007. The field has reverted to its natural status in the past 50 years. Similar to the site of Hao et 10 al.(2007), the xeric rhizomatous grass Leymus chinensis is the constructive species, and 11 12 Agropyron cristatum, Cleistogenes squarrosa, and Carex duriuscula are the dominant species at our site. The heights of grass clumps are about 0.50-0.70 m, and coverage fraction 13 depends on annual precipitation, ranging from 30% to 70%. Soil at the site was 14 predominantly dark chestnut (Mollisol) soil with rapid drainage of water. It has only a thin 15 layer of humus (the organic portion of the soil created by partial decomposition of plant or 16 17 animal matters) which provides vegetation with nutrients.

This site is smooth, homogeneous and approximately 1500 m \times 1500 m, surrounded by low hills whose heights are lower than 30 m with slopes less than 5°. Unfortunately, the leaf area index (LAI) has not been measured. This site has a semi-arid continental temperate steppe climate with a dry spring, autumn, humid summer and snow-covered winter. The average annual temperature is about 272.5 K, with a growing season of 150-180 days. The

annual precipitation range is 320-400 mm, and rainfall is concentrated within the period
 from June to August (Hao et al., 2007).

3 2.2 Micrometeorological measurements

4 *(i) Fast response measurements.*

5 A three-dimensional sonic anemometer (CSAT3, Campbell Scientific Inc.) was used to measure the means and standard deviations of wind velocity components (i.e., u, v and 6 7 w) and air temperature (T), and a LI-7500 (LiCor, USA) gas analyzer was used to measure the mean and standard deviations of water vapor density and CO_2 . The gas analyzer was 8 calibrated before the experiment using three values of standard gases (between 300 and 400 9 ppmv CO_2 in N_2). These sensors were installed on a mast at 4.0 m above the ground 10 (Figure 1). The sensor outputs were recorded at a sampling rate of 10 Hz and were 11 12 averaged over 30 min periods. Appropriate corrections were made for non-zero mean vertical velocity. Following Moore (1986), we corrected eddy covariance values for the 13 effects of path length averaging of the sonic anemometer and the gas analyzer, and for the 14 spatial separation of sensors. Corrections were made for density fluctuations in calculating 15 16 the fluxes of water vapor and CO_2 (Webb *et al.*, 1980).

We eliminated outliers from 30-min measurements of turbulence by using a criterion of $X(t) < (\overline{X} - 4 \sigma)$ or $X(t) > (\overline{X} + 4\sigma)$, where X(t) denotes the measurement (i.e., wind speed components, temperature), \overline{X} is the mean over the interval and σ the standard deviation. Data during and after rain events was removed because the sonic anemometer could malfunction in these cases. The gaps shorter than a half hour were filled by linear interpolation.

(ii) Slow response measurements 1

2	Other supporting data were collected during the experiment. Soil heat flux was
3	measured by embedding two heat flux plates (HFT-3, Campbell Scientific Inc.) at a depth of
4	0.01 m. Soil temperature was measured at 6 depths (surface, 0.05 m, 0.10 m, 0.15 m, 0.20 m,
5	and 0.40 m) in the soil. Upward and downward short- and long-wave radiation components
6	were measured with radiometers (model 2AP Tracker, Kipp & Zonen Inc.) mounted at a
7	height of 2.0 m. The data were recorded by a Datataker (CR5000, Campbell Scientific Inc.)
8	with a PCMCIA memory card. The data were sampled each minute and averages recorded
9	every 10 min.
10	The set of observational data includes the following meteorological quantities:
11	horizontal wind speed, air temperature, specific humidity, air pressure and precipitation.
12	Figure 2 shows the time series of (a) weekly mean wind vector (WV in m s ⁻¹), (b) weekly
13	mean air temperature (Tair in K), (c) weekly mean specific humidity (q in g kg ⁻¹), (d) daily
14	mean air pressure (P in hpa), and (e) daily precipitation (Prec. in mm day ⁻¹) obtained since
15	June 2007. It is obvious that all of these meteorological quantities undergo a marked
16	seasonal cycle. In the wet season (June through August), high temperature, high humidity,
17	and low wind speed were coincident with low air pressure and precipitation events were
18	frequent. The reverse occurred during the dry season.
19	The plots in Figures 2a 2c are derived from the fast response measurements. The
20	composition method is applied for estimation of daily variation for each week and then a

weekly average is calculated. The gaps in Figure 2 were caused by power outages at the site. 21

The plots in Figures 2d-2e are derived from the slow response instruments. 22

1	
1	Our site is located in a mid latitude semi arid continental temperate and westerlies
2	climate zone. During the winter, cold dry air always came from the southwest, significantly
3	influencing the area. Because of the influence of the temperate monsoon climate, the south
4	to southwest wind was maintained through whole experimental period. Although the annual
5	mean wind speed was about 3.0 m s ⁻¹ (shown in Figure 2a), the maximum hourly mean
6	wind speed reached 8 m s ⁻¹
7	The seasonal variation of air temperature (Tair) was remarkabledramatic. Monthly
8	mean air temperature reached a maximum (295.0 K) in July and August, and the lowest air
9	temperature (252.0 K) occurred in the middle of December. The difference between the
10	highest air temperature and lowest air temperature was 43 K for the whole experimental
11	period and the annual mean air temperature was 277.5 K. Similar seasonal variation
12	occurred in specific humidity (q), with the correlation coefficient between q and Tair
13	reaching 0.82. Specific humidity varied also in response to variations in precipitation
14	(Figure 2c and 2c). Because of the semi-arid continental temperate climate, q is always less
15	than 12 g kg ⁻¹ , and less than 5 g kg ⁻¹ during the period from October 2007 to April 2008.
16	Air pressure varied seasonally but in reverse phase to air temperature and specific
17	humidity. Almost all precipitation occurred from June to August 2007 and in June 2008.
18	Snow occurred during the periods: 2-10 December, 2007, 21, 29 January, and 15, 24, 27-30

19 March, 2008.

- 20 2.3 Theoretical Considerations
- 21

The surface energy balance over the grass canopy can be approximated by:

$$Rn = H + LE + G_0 + \operatorname{Re}, \qquad (1)$$

where Rn is the net radiation, H and LE are the sensible heat and latent heat fluxes, respectively, G_0 is the soil heat flux at the surface, and Re is the residual energy involved in various processes, such as photosynthesis and respiration (Harazono *et al*, 1998, Burba *et al.* 1999). We determine Re from the formula: Re = $Rn - (H + LE + G_0)$. R_n was measured using slow response instruments (described above). Eddy fluxes of sensible heat and latent heat were calculated as (e.g., Kaimal and Finnigan, 1994):

$$H = \overline{\rho}C_{p} \overline{w'T'}, \qquad (2)$$

7

$$LE = L\overline{\rho}w'q',\tag{3}$$

9 where $\overline{\rho}$, C_p and L are the density of air (kg m⁻³), the specific heat of air (J kg⁻¹ K⁻¹), 10 and the latent heat of vaporization (J kg⁻¹), respectively. w', T' and q' are the 11 fluctuations in the vertical wind component (m s⁻¹), air temperature (K) and specific 12 humidity, respectively.

 G_0 is estimated by using a combination of soil calorimetry and measurement of the heat flux density at depth of 0.1 m using heat flow transducers. The heat storage of the soil layer above the plate is included as follows,

16

$$G_0 = G_1 + C_g \Delta z \,\delta T \,/\, \delta t \,, \tag{4}$$

where G_1 is the soil heat flux at depth of 0.1 m, Cg the volumetric heat capacity of the soil, which can be easily derived from soil components (Gao, 2005), Δz the thickness of a thin layer of the soil, *T* the mean soil temperature of the thin layer, δT the change in mean soil temperature during the measurement period, and δt the change in time.

Since the 1980s, the development of fast response CO_2 analyzers has enabled us to directly measure CO_2 fluxes over rice canopies using eddy covariance methods:

$$F_c = \overline{w'c'},\tag{5}$$

2 where F_c is CO_2 flux (mg m⁻² s⁻¹) and c' is the fluctuation in the concentration of CO_2 3 (mg m⁻³) (Desai *et al.*, 2008).

4 The ratio of the sum of sensible and latent heat fluxes (H + LE) to available energy (the 5 difference of net radiation and soil heat flux: $Rn - G_0$) is presented to examine the surface 6 heating rate ε .

Horst and Weil (1994) documented the stability dependency of footprint. The adequacy of the fetch may be confirmed by footprint analysis for neutral flow(e.g. Schuepp *et al.*, 1990, and Harazono *et al.* 1998). The cumulative normalized contribution to the surface flux from upwind locations, $C_F(\chi_L)$, can be expressed as

$$C_F(\chi_L) = \exp[-U(z-d)/ku_*\chi_L], \qquad (6)$$

where d is the zero plane displacement, k is von Karman's constant, u_* is the friction 12 velocity, χ_L is the distance upwind of the measuring point, and U is the average wind 13 speed between the surface and observation height z. Assuming a logarithmic profile for 14 horizontal wind with 15 speed u(z)z , Uis given by $U = \int_{d+z_0}^{z} u(z) dz / \int_{d+z_0}^{z} dz = \frac{u_* [\ln((z-d)/z_0) - 1 + z_0/(z-d)]}{k(1-z_0/(z-d))}$. The code from Schmid *et al* (1994) is 16 publicly available (http://www.indiana.edu/~climate/SAM/SAM_FSAM.html) and was used 17 in this study. 18

19

11

1

20 3. Results and Discussion

21 <u>The set of observational data includes the following meteorological quantities:</u>
 22 <u>horizontal wind speed, air temperature, specific humidity, air pressure and precipitation.</u>

1	Figure 2 shows the time series of (a) weekly mean wind vector (WV in m s ⁻¹), (b) weekly
2	mean air temperature (Tair in K), (c) weekly mean specific humidity (q in g kg ⁻¹), (d) daily
3	mean air pressure (P in hpa), and (e) daily precipitation (Prec. in mm day ⁻¹) obtained since
4	June 2007. It is obvious that all of these meteorological quantities undergo a marked
5	seasonal cycle. In the wet season (June through August), high temperature, high humidity,
6	and low wind speed were coincident with low air pressure and precipitation events were
7	frequent. The reverse occurred during the dry season.
8	The plots in Figures 2a-2c are derived from the fast response measurements. The
9	composition method is applied for estimation of daily variation for each week and then a
10	weekly average is calculated. The gaps in Figure 2 were caused by power outages at the site.
11	The plots in Figures 2d-2e are derived from the slow response instruments.
12	Our site is located in a mid-latitude semi-arid continental temperate and westerlies
13	climate zone. During the winter, cold dry air always came from the southwest, significantly
14	influencing the area. Because of the influence of the temperate monsoon climate, the south
15	to southwest wind was maintained through whole experimental period. Although the annual
16	mean wind speed was about 3.0 m s ⁻¹ (shown in Figure 2a), the maximum hourly mean
17	wind speed reached 8 m s ⁻¹
18	The seasonal variation of air temperature (Tair) was remarkable. Monthly mean air
19	temperature reached a maximum (295.0 K) in July and August, and the lowest air
20	temperature (252.0 K) occurred in the middle of December. The difference between the
21	highest air temperature and lowest air temperature was 43 K for the whole experimental
22	period and the annual mean air temperature was 277.5 K. Similar seasonal variation

occurred in specific humidity (q), with the correlation coefficient between q and Tair 1 reaching 0.82. Specific humidity varied also in response to variations in precipitation 2 (Figure 2c and 2e). Because of the semi-arid continental temperate climate, q is always less 3 than 12 g kg⁻¹, and less than 5 g kg⁻¹ during the period from October 2007 to April 2008. 4 Air pressure varied seasonally but in reverse phase to air temperature and specific 5 humidity. Almost all precipitation occurred from June to August 2007 and in June 2008. 6 Snow occurred during the periods: 2-10 December, 2007, 21, 29 January, and 15, 24, 27-30 7 March, 2008. The snow amounts were not measured. 8

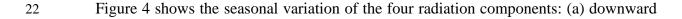
9 3.1 Footprint Analysis

10 Data were collected at 4 m above the ground surface, which is higher than three times of the maximum height (0.6 m) of the grass clumps on the Steppe. Thus the flow assumes 11 12 the properties of the conventional atmospheric surface layer such as the constant flux region. To estimate the average footprint for whose experiment, the contributions of the cumulative 13 flux were computed using Equation (6), where U = 3.98 m s⁻¹, z = 4.0 m, d = 0.2 m, 14 and $u_* = 0.30$ m s⁻¹. Our analysis (Figure 3) indicates that approximately 90% of the 15 measured flux at the measurement height was expected to come from within the nearest 16 1100 m of upwind area for neutral stability during the entire period. The footprint flux 17 distribution shows the maximum source weight location is 60 m upwind from the mast. 18

19

20 3.2 Seasonal Variations on a Weekly Average Basis

21 3.2.1 Radiation Components



shortwave radiation (hereinafter, referred to as DSR), (b) upward shortwave radiation (USR), 1 (c) downward longwave radiation (DLR), (d) upward longwave radiation (ULR), and (e) 2 3 albedo of the underlying surface, defined as the ratio of the maximum values of USR and DSR. The seasonal variations of DSR, DLR and ULR were similar. They maintained high 4 values during the summer and low values during the winter. The seasonal variation of USR 5 had not been obvious when ground was not snow-covered and the seasonal variation of 6 albedo was relatively constant at 0.22. After snow occurred, USR increased and the albedo 7 drastically increased increased dramatically. 8

9

The consistent seasonal variation Tair, q, P, Prec., DSR, DLR, and ULR are shown in Figures 2 and 4. 10

3.2.2 Energy Components and CO₂ flux 11

12 Figure 5 shows the seasonal variation of weekly means of (a) net radiation (Rn), (b) 13 sensible heat flux (H), (c) latent heat flux (LE), (d) soil surface heat flux (G_0), and (e) CO_2 flux (F_{CO_2}). Rn was calculated by using the four radiation components (i.e., DSR, 14 USR, DLR, and ULR). H, LE and F_{CO_2} were measured by fast response instruments 15 and calculated using Equations (2, 3 and 5). Gaps occurring in H, LE, G_0 and F_{CO_2} 16 were caused by instrument problems. 17

18 Rn, H, LE, G_0 , and F_{CO_2} all showed remarkable seasonal variation. The negative sign in F_{CO_2} means that surface vegetation absorbed CO_2 . The variations in Rn, H, LE, 19 G_0 and F_{CO_2} are generally consistent; however the weekly oscillation in LE was 20 weaker than those in Rn, H, and F_{CO_2} . The sensible heat flux was the main consumer of 21 surface available energy $(Rn - G_0)$. The grass grew well in the summer, and the strong 22

photosynthesis led to the larger water vapor release and the larger negative F_{CO_2} . G_0 was about several watts per square meter on average. During December 2007 when ground was covered by snow: (1) Rn was negative; (2) the grass was short and senescent, and CO_2 absorption therefore decreased; (3) the snow surface absorbed sensible heat flux from the air; (4) *LE* was close to zero; and (5) G_0 was almost constant (negative several watts per square meters).

7 3.3 Diurnal Variations on Monthly Average Basis

8 3.3.1 Radiation Components

9 In order to investigate the diurnal variation of the radiation components, the monthly means of the diurnal variation in the radiation components (DSR, USR, DLR, and ULR) are 10 given in Figure 6 where a composite analysis method is used and the short lines are error 11 12 bars. We find that diurnal variations in DSR, USR and ULR occurred in all months, whereas diurnal variations in DLR were not significant from November 2007 to February, 2008. 13 Diurnal variations in DSR and ULR were largedramatic in summer, but weaker in winter. 14 15 On average, the maximum values of DSR and ULR occurred in June 2007 and reached 804.4 W m⁻² and 558.1 W m⁻² respectively. The minimum values of DSR and ULR occurred 16 in December 2007, and reached 354.9 W m⁻² and 264.7 W m⁻² respectively. The maximum 17 value of DLR occurred in July 2007, and reached 371.2 W m⁻². The maximum value of USR 18 occurred in February 2008 and reached 257.8 W m⁻² and the minimum value of USR 19 occurred in November 2007 and reached 144.4 W m⁻². The large USR occurring from 20 December 2007 through February 2008 were caused by large albedo of the snow-covered 21 surface, resulting in the large surface albedo shown in Figure 6e. It is a clear indication that 22

1 the albedo of fresh snow was higher than 0.64.

2

22

3 3.3.2 Energy Components

The monthly mean diurnal variation courses of net radiation (Rn), sensible heat flux 4 (*H*), latent heat flux (*LE*), soil heat flux (G_0), and CO_2 flux (F_{CO_2}) for all <u>334 sunny</u> 5 clear days during this 390-day observation period are given in Figure 7 where a composite 6 7 analysis method is used and the short lines are error bars. Figure 7a shows that the diurnal variation pattern of Rn is similar to that of DSR, i.e., the diurnal variation was significant 8 9 in summer and weak in winter. The maximum diurnal variation occurred in July and the peak value of Rn reached 488.8 W m⁻². The minimum diurnal variation occurred in 10 January 2008 and the peak value of Rn was 115.3 W m⁻². 11

Figure 7b shows that seasonal variations in sensible heat flux were stronger than those in *LE*. The maximum value of *H* occurred in May 2008 and reached 302.6 W m⁻² and the minimum value of *H* occurred in December 2007 and was 54.4 W m⁻².

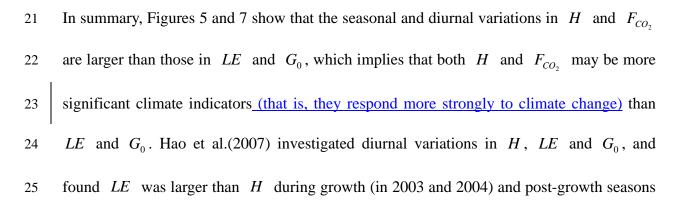
Figure 7c shows that the seasonal variation in latent heat flux was remarkable. Obvious diurnal variation of *LE* occurred in summertime, with a maximum value of 106.8 W m⁻² occurring in June 2008. Diurnal variation of *LE* was not significant in wintertime and the maximum value was 30.0 W m⁻² which occurred in January 2008. Obvious diurnal variation of *LE* in summer might be attributed to the following: (1) precipitation frequently occurred (as shown in Figure 2) and steppe grass grew well in summer, and (2) the diurnal variation in net radiation was large in summer (as shown in Figure 7a).

____Figure 7d shows the seasonal variation of soil surface heat flux (G_0). Hao et al.(2007)

1 estimated soil heat flux by averaging the output of two heat flux plates buried investigated the soil heat flux measured at 0.05 m depth and did not findfound obvious diurnal variations 2 3 in their selected four periods (i.e., pre-growth, growth, post-growth, and frozen soil) at their 4 steppe site in Inner Mongolia as shown in their Figure 4. However, these diurnal variations in soil heat flux were weaker than those in sensible and latent heat fluxes. - Our Figure 7d 5 shows that there is significant diurnal variation in G_0 . The difference of our results from 6 7 those by Hao et al. (2007) can be attributed to two facts: (1) Hao et al. (2007) neglected the 8 soil heat storage in the soil layer <u>extending</u> from <u>the</u> surface to 0.05 m depth. Our analysis shows that the soil heat storage in thise shallow surface layer varied diurnally changed on 9 sunny clear-days; and (2) we selected only clear-sunny days for analysis, but Hao et al. 10 11 (2007) used all data for their investigation. Soil heat flux is very low or questionable on rainy or cloudy days. 12

Figure 7e shows that the seasonal variation of F_{CO_2} was similar to that of H and LE, but of opposite signin the reverse phase. The most significant diurnal variation occurred in May 2008 when the steppe grass was luxuriant. The peak value reached -0.69 mg m⁻² s⁻¹. Weak diurnal variation occurred in December 2007 when the grass was mostly senescent and the peak value was only -0.21 mg m⁻² s⁻¹. This small carbon in the winter was probably the result of some grass still living in the winter.

- 19
- 20



(in 2004). The reason is that precipitation was frequent in 2003 and 2004, which can be seen 1 in their Fig. 2, and precipitation caused high surface evaporation in their experiment areas. 2 Bi et al. (2007) examined energy partitioning and CO2 exchange over grassland in 3 the tropical monsoon environment of southern China by using H, LE, and F_{CO_2} measured 4 5 in the near-surface layer from May 2004 to July 2005. In contrast to our results, Tthey found that both LE and F_{CO_2} may be more significant climate indicators than H and G_0 in 6 that area. Thus, surface turbulent fluxes in different climate zones in China respond to climate 7 8 change in different ways.

9

10 **3.4 Energy Partitioning**

11 The monthly means of the Bowen ratio ($\beta \equiv H/LE$) were 3.25, 3.25, 3.28, 3.34, 3.44, 3.49, 12 3.56, 3.61, 3.54, 3.41, 3.32, 3.25 and 3.21 from June 2007 to June 2008. It is obvious that

the Bowen ratio was almost constant and did not vary monthly, which suggests partitioning surface

14 available energy $(Rn - G_0)$ into sensible and latent heat flux by <u>assuming a constant Bowen ratio</u>.

15 ($Rn - G_0$) can be observed by using slow response instruments as mentioned above. It is

<u>also</u> obvious that the sensible heat flux was the main consumer of available energy $(Rn - G_0)$ 16 for all the year round in this arid and semiarid area. Taking a yearly average, the Bowen 17 ratio was 3.38, H/Rn = 62%, LE/Rn = 18%, $G_0/Rn = 9\%$, and Re/Rn = 11%. Because the 18 19 site was covered by grass, the residual energy (Re) is mainly the heat storage in the grass. The proportion of sensible heat flux in net radiation, H/Rn reached the maximum value 20 (0.63) in June through August 2007 and May through June in 2008 and reached the 21 22 minimum value of 0.61 in December 2007. H/Rn was lower than 0.62 during the period from October 2007 to February 2008, and was larger than 0.62 during summer 2007. 23 The proportion of latent heat flux in net radiation, LE/Rn, reached a maximum value (0.19) 24 in June 2008, and reached a minimum value (0.17) in January 2008. LE/Rn was less than 25 0.18 during the period from October 2007 through February 2008, and was larger than 0.18 26 for the rest of the time. 27

Figure 8 shows the intercomparison of H + LE and $Rn - G_0$. The surface heating

1 rate ε is 0.93 and the correlation coefficient between H + LE and $Rn - G_0$ is 0.85. 2 Wever et al. (2002) examined the energy balance over a northern temperate grassland near 3 Lethbridge, Alta., Canada, and found that the slope of the relationship between H + LE4 and $Rn - G_0$ ranged from 0.87 to 0.90. Hao et al.(2007) used soil heat flux measured at 5 0.05 m depth rather than soil surface heat flux for energy balance analysis, and found that 6 H + LE = 0.69(Rn - G) + 17.09. Their failure to close the energy budget may be partly 7 attributed to neglecting soil and vegetation heat storage.

8

10

Our analysis of the surface heating rate is focused on the data collected on rain-freesunny days, because the sonic anemometer malfunctions during and after rain events.

Theoretically, ε should be very close to 1.0. The energy imbalance that occurred for 11 12 these measurements is unexpected because the experiment was carried out over a relatively flat, homogeneous site with sufficient fetch and the flux calculations are rigorous. Such 13 energy imbalances have also been encountered in other major field campaigns and caused 14 difficulty for their climate applications (e.g. Kahan et al., 2006). Previous researchers 15 (Foken and Oncley, 1995; Panin et al., 1996; Wicke and Bernhofer, 1996; Foken et al., 1999; 16 Kahan et al., 2006; Oncley et al., 2007; Su et al., 2008) concluded that the causes of the 17 imbalance of the energy budget were usually related to the errors/uncertainties in the 18 individual energy component measurements and the influence of different footprints on the 19 individual energy components. For our site, the difference in phases of Rn, H, LE and 20 G_0 (Gao et al., 2009), and the unavoidable uncertainties that occurred in the individual 21 energy component measurements are the main causes of the energy imbalance encountered. 22

1

2 **3.5 Soil Temperature**

Surface radiation and energy budget balances are related to variations in soil temperature and soil water content. Figure 9 shows the seasonal variation of half-hourly-mean soil temperatures at soil surface and five depths (0.05 m, 0.10 m, 0.15 m, 0.20 m, and 0.40 m), and water content at three depths (0.10 m, 0.20 m, and 0.50 m). The seasonal variation trends of soil temperature and water content are close to that of air temperature. The soil surface temperature is derived from ULR where the infrared emissivity is assumed to be 0.98 (Garratt, 1992).

As may be expected, the seasonal variations in soil temperature and water content in 10 shallow layers were large. There is evidence of seasonal variation in soil temperature measured 11 12 at 0.40 m depth. In general the range of seasonal variations measured in the deep layer was much less than those of soil temperature and water content measured in the shallower layers. 13 The high soil temperatures occurred during summer (June - August), and low soil 14 temperature occurred in January and February. The difference between the annual highest 15 and lowest soil temperature ranged from 38 K to 59 K for these depths. Soil water content at 16 17 0.10 m depth sensitively responded to precipitation with the most striking case happening on August 3 2007 when a thunderstorm made the greatest sudden change of soil wetness. 18

We also examined the diurnal variation of soil temperatures. Results show that soil temperatures diurnally changed in shallow layers, diurnal variation trends weakened with increasing depth and almost no diurnal variation occurred with soil temperature measured at a depth of 0.4 m. 1

2 **3.6 Case Study of Diurnal Cycles**

In this section we investigate the diurnal cycle of the radiation components, energy fluxes, CO_2 flux, and energy balance for <u>clear dayssunny days</u> under specific shortwave radiation environments: (1) on June 7 2008, the daily downward shortwave radiation reached the largest value of our experimental period; and (2) On December 22 2007, the albedo daily upward shortwave radiation reached the largest value of our experimental period. Figure 10 shows the diurnal cycle of radiation components for these two days, and the corresponding daytime surface albedo.

The maximum values of downward shortwave radiation and upward shortwave radiation were 1020 W m⁻² and 229 W m⁻², respectively, on June 7 2008; 424 W m⁻² and 304 W m⁻², respectively, on December 22 2007. The corresponding surface albedo values were 0.22 and 0.70 <u>on June 7 2008 and December 22, 2007, respectively</u>. The winter surface albedo is higher than the summer surface albedo because of snowfall.

15 The downward longwave radiation components on June 7 2008 were greater than those on December 22 2007, and both of them showed almost no daily change. The upward 16 shortwave radiation component on June 7 2008 diurnally changed in contrast to that on 17 December 22 2007. Similar to Figure 10, the daily cycles of the energy flux components and 18 CO₂ flux for the two days mentioned above were plotted in Figure 11. The maximum values 19 of net radiation (*Rn*), sensible heat (*H*), latent heat (*LE*), soil heat (G_0), and CO_2 (F_{CO_2}) 20 fluxes were 564.0 W m². 294.5 W m². 141.9 W m². 168.1 W m² and 0.63 mg m² s⁴ on 21 June 7 2008. The maximum values of -Rn, -H, -LE, $-G_0$, and $-F_{CO_2}$ were 34.0 W m², 22

1 $\begin{bmatrix} 20.2 \text{ W m}^2, 9.8 \text{ W m}^2, 19.2 \text{ W m}^2 \text{ and } 0.07 \text{ mg m}^2 \text{s}^4 \text{ on December 22 2007. On June 7} \\ 2 2008, the sensible heat flux was larger than the latent heat flux; and on December 22 2007, \\ 3 the sensible heat flux and latent heat flux were close to zero. On June 7 2008, the daytime \\ 4 CO_2 absorption was significant because of the strong photosynthesis associated with the$ $5 grass, and on December 22 2007, the daytime CO_2 absorption was close to zero owing to$ 6 snow-covered surface.

Figure 12 shows the energy partitioning for June 7 2008 and December 22 2007.
Sensible heat fluxes were 90.3 W m⁻² and -17.4 W m⁻²; latent heat fluxes were 58.2 W m⁻²
and -0.71 W m⁻²; soil heat fluxes were 21.9 W m⁻² and -5.8 W m⁻²; and residual heat fluxes
were -3.2 W m⁻² and -12.4 W m⁻² for June 7 2008 and December 22 2007 respectively.

- 11
- 12 **4.**

4. Summary and Conclusions

In order to investigate energy partitioning and CO_2 exchange over the land surface in a northern arid climate environment and to investigate which surface energy components are strong climate signals, eddy covariance measurements of moisture, heat and CO_2 fluxes over steppe prairie in Inner Mongolia, China were carried out from June 2007 through June 2008.

All four radiation components seasonally changed, resulting in a seasonal variation in net radiation. The components also changed diurnally. Winter surface albedo was higher than summer surface albedo, because in winter the surface was covered by snow.

Appropriate correction was made for turbulent fluxes. The seasonal variations in both sensible heat and CO_2 fluxes were stronger than those in latent heat and soil heat fluxes, which implies that both sensible heat and CO_2 fluxes may be more significant climate signals than latent heat and soil fluxes. Sensible heat flux was the main consumer of available energy for the entire experimental period.

Surface energy partitioning was examined and the surface heating rate (ε) was found to be 0.93 during the experiment. The energy imbalance problem was encountered. The main causes of the energy imbalance encountered were thought to be the difference in phases of Rn, H, LE and G_0 (Gao *et al.*, 2009), and the unavoidable uncertainties that occurred in the individual energy component measurements.

9

10 Acknowledgments

supported by MOST (2006CB400600, This study was mainly 11 12 2006CB403500, 2006BAB18B03, and 2006BAB18B05), by CMA (GYHY(QX)2007-6-5), by NSFC (40233032), and by the Centurial Program 13 sponsored by the Chinese Academy of Sciences. The work described in this 14 publication was also supported by the European Commission (Call FP7-ENV-2007-1 15 Grant nr. 212921) as part of the CEOP – AEGIS project (http://www.ceop-aegis.org/) 16 17 coordinated by the Université Louis Pasteur. The National Center for Atmospheric 18 Research is sponsored by the National Science Foundation. We are very grateful to the anonymous reviewer for a careful review and valuable comments, which led to 19 substantial improvement of this manuscript. 20

21

22

References

Э	
6	Adams J. M., Faure H., Faure-Denard L., McGlade J. M., and Woodward F. I.: Increases in
7	terrestrial carbon storage from the Last Glacial maximum to the present. Nature 348, 711-714,
8	1990.
9	Baldocchi D. D., and Vogel C. A.: Seasonal variation of energy and water vapor exchange rates
10	above and below a boreal jack pine forest canopy, Journal of Geophysical Research, 102. D24,
11	28,939-28,951, 1997.
12	Baldocchi D. D., Vogel C. A., and Brad H.: Seasonal variation of carbon dioxide exchange rates
13	above and below a boreal jack pine forest. Agric. For. Meteorol. 83, 147–170, 1997.
14	Baldocchi D. D., Falge, E., and Gu, L. H., et al. : Fluxnet: A new tool to study the temporal and
15	spatial variability of ecosystem-scale carbon dioxide, water vapor, and energy flux densities. Bull.
16	Am.Meteorol. Soc. 82, 2415–2434, 2001.
17	Barros A. P., Munoz F., Wood A. W., Voisin N., Bohn T., Rodriguez J. C., Lettenmaier D. P.,
18	Burges S. S., and Watts C. J.: Monitoring the diurnal cycle of land-atmosphere interactions in
19	Sonora, Mexico during NAME/SMEX04, AMS Conference on Hydrology. 19, 2005.
20	Beljaars A. C. M., and Holtslag A. A. M.: Flux parameterization over land surfaces for atmospheric
21	models. J. Appl. Meteor., 30, 327-341, 1991.
22	Betts A. K., and Ball J. H.: The FIFE surface diurnal cycle climate, Journal of Geophysical

1 Research,	100(D12),	679-693,	1995.
-------------	-----------	----------	-------

2	Bi X., Gao Z., Deng X., Wu D., Liang J., Zhang H., Sparrow M., Du J., Li F., and Tan H.: Seasonal
3	and diurnal variations in moisture, heat and CO_2 fluxes over grassland in the tropical monsoon
4	region of southern China, J. Geophys. Res. 112, D10106, doi: 10.1029/2006JD007889, 2007.
5	Burba G. G., Verma S. B., and Kim J.: Surface energy fluxes of Phragmites australis in a prairie
6	wetland, Agricultural and Forest Meteorology, 94, 31-51, 1999.
7	Campbell C. S., Heilman J. L., McInnes K. J., Wilson L. T., Medley J. C., Wu G. W., and Cobos D.
8	R.: Diel and seasonal variation in CO ₂ flux of irrigated rice, Agricultural and Forest Meteorology
9	1, 108, 1527, 2001.
10	Chen Z. Z., Wang S. P., and Wang Y. F.: Update progress on grassland ecosystem research in Inner
11	Mongolia steppe, Chinese Bull. Botany, 20, 423-429, 2003.
12	Delire C, and Gerard J. G.: A numerical study of the influence of the diurnal cycle on the surface
13	energy and water budgets. Journal of Geophysical Research, 100(D3), 5071-5084, 1995.
14	Desai A. R., Noormets A. N., Bolstad P. V., Chen J., Cook B. D., Davis K. J., Euskirchen E. S.,
15	Gough C.M., Martin J. G., Ricciuto D. M., Schmid H. P., Tang J. W. and Wang W.: Influence of
16	vegetation and surface forcing on carbon dioxide fluxes across the Upper Midwest, USA:
17	Implications for regional scaling, Agricultural and Forest Meteorology,
18	doi:10.1016/j.agrformet.2007.08.001, 2008.
19	Dickinson R. E., Hendersin-Sellers A., Rosenzweig C., and Sellers P. J.: Evapotranspiration models
20	with canopy resistance for use in climate models, a review, Agric. For. Meteorol., 54, 373-388,
21	1991.
22	Dugas W. A., Heuer M. L., and Msyeux H. S.: Carbon dioxide fluxes over Bermuda grass, native

23 prairie, and sorghum. *Agricul. For. Meteorol.* 93, 121–139, 1999.

1	Foken T. and Oncley S. P. : 'Results of the workshop "Instrumental and methodical problems of
2	land surface flux measurements"", - Bull. Am. Meteorol. Soc. 76, 1191-1193, 1995.
3	Foken T., Kukharets V. P., Perepelkin V. G., Tsvang L.R., Richter S. H., and Weisensee U.: 'The
4	influence of the variation of the surface temperature on the closure of the surface energy balance',
5	- 13th Symposium on Boundary Layer and Turbulence, Dallas, TX., 10-15 Jan. 1999, Amer.
6	Meteorol. Soc, 308-309, 1999.
7	Frank A.B., and Dugas W. A.: Carbon dioxide fluxes over a northern, semiarid, mixed grass prairie.
8	Agricul. For. Meteorol. 108, 317-326., 2001.
9	Gao Z., Bian L. and X. Zhou.: Measurements of Turbulent Transfer in the Near-surface Layer over a
10	Rice Paddy in China, J. Geophys. Res. 108(D13), 4387, dio: 10.1029/2002JD002779, 2003.
11	Gao Z.: Determination of soil heat flux in a Tibetan short-grass prairie, Boundary-Layer
12	Meteorology, 114, 165-178, 2005.
13	Gao Z., Horton R., Liu H. P., Wen J., Su. Z. B., and Wang L.: Influence of wave phase difference
14	between surface soil heat flux and soil surface temperature on land surface energy balance
15	closure, Hydrology and Earth System Sciences, submitted.
16	Garratt J. R.: The Atmospheric Boundary Layer, Cambridge University Press, Cambridge, 316 pp,
17	1992.
18	Hao Y., Wang Y., Huang X., Cui X., Zhou X., Wang S., Niu H., and Jiang G.: Seasonal and
19	interannual variation in water vapor and energy exchange over a typical steppe in Inner Mongolia,
20	China, Agricul. For. Meteorol. 146, 57-69, 2007.
21	Harazono Y., Kim J., Miyata A., Choi T., Yun J. –I. and Kim J. –W.: Measurement of energy budget
22	components during the International Rice Experiment (IREX) in Japan, Hydrological Processes,

1	12,	2018	-2092,	1998.
---	-----	------	--------	-------

- 2 Hartog G. D., and Neumann H. H., Energy budget measurements using eddy correlation and Bowen
- 3 ratio techniques at the Kinosheo Lake tower site during the Northern Wetlands Study, *Journal of*
- 4 *Geophysical Research*, vol.99, No. D1, 1539-1549, 1994.
- 5 Horst T. W., and Weil J.C.: How far is far enough?: The fetch requirements for micrometeorological
- 6 <u>measurement of surface fluxes</u>. J. Atmospheric Oceanic Technology, **11**, 1019-1025, 1994.
- 7 Intergovernmental Panel on Climate Change, Climate Change 1995: The Science of Climate Change.
- 8 In: Houghton, J. T., Meira Filho, L. G., Callander, B. A., Harris, N., Kattenberg, A., Maskell, K.
- 9 (eds.), Cambridge Univ. Press, New York, 1995.
- 10 Kahan D. S., Xue Y., and Allen S. J.: The impact of vegetation and soul parameters in simulations of
- 11 surface energy and water balance in the semi-arid sahel: A case study using SEBEX and

12 HAPEX-Sahel data, Journal of Hydrology, 320, 238-259, 2006.

- 13 Kaimal J. C., and Finnigan J.: Atmospheric Boundary Flows, Their Structure and Measurement,
- 14 Oxford Univ. Press, New York, 1994.
- 15 Li S., Werner E., Asanuma J., Kotani A., Davaa G., Dambaravjaa, O. and Michiaki S.: Energy
- 16 partitioning and its biophysical controls above a grazing steppe in central Mongolia. *Agricul. For.*
- 17 *Meteorol.* 137, 89-106, 2006
 - Merquiol E., Pnueli L., Cohen M., Simovitch M., Rachmilevitch S., Goloubinoff P., Kaplan A, and Mittler R.: Seasonal and diurnal variations in gene expression in the desert legume Retama raetam, *Plant, Cell and Environment*, 25, 1627-1638, 2002.
 - Mielnick, P. C., Dugas W. A., Johnson H. B., Polley H. W., and Sanabria J.: Net grassland carbon flux over a subambient to superambient CO₂ gradient, *Global Change Biology*, 7, 747-754,

- Moore C. J.: Frequency response to corrections for eddy correlation system. *Bound.-Layer Meteor.*, **37**. 17-35, 1986.
- Novick K. A., Stoy, P. C., Katul, G. G.: Carbon dioxide and water vapor exchange in a warm temperate grassland. *Oecologia*, 138, 259-274, 2004.
- Oncley, S. P., Foken T., Vogt R., Kohsiek W., DeBruin H. A. R., Bernhofer C., Christen A., van Gorsel E., Grantz D., Feigenwinter C., Lehner I., Liebethal C., Liu H., Mauder M., Pitacco A., Ribeiro L., Weidinger T. : The energy balance experiment EBEX-2000. Part I: overview and energy balance, *Boundary-Layer Meteorol*. 123:1–28, DOI 10.1007/s10546-007-9161-1, 2007.
- Panin G. N., Tetzlaff G., Raabe A., Schönfeld H. J., Nasonov A. E.: 'Inhomogeneity of the land surface and the parametrization of surface fluxes - a discussion', Wiss. Mitt. aus dem Inst. für Meteorol. der Univ. Leipzig und dem Institut für Troposphärenforschung e.V. Leipzig, 4, 204-215, 1996.
- Rowntree P. R.: Atmospheric parameterization schemes for evaporation over land: basic concepts and climate modeling aspects, in Land Surface *Evaporation. Measurement and Parameterization*, edited by T. J. Schmugge and J. C. Andre, 5-29., Springer-Verlag, New York, 1991.
- Schmid H. P.: Source areas for scalars and scalar fluxes, *Boundary-Layer Meteorology*, 67, 293-318, 1994.
- Schuepp P. H., Leclerc M. Y., MacPherson J. I. and Desjardins R. L.: Footprint prediction of scalar fluxes from analytical solution of the diffusion equation. *Bound.-Layer Meteor.*, **50**, 355-373,

1990.

1

2

3

Λ	leteorol. 109, 117-134, 2001.
Stev	en J. H., Walter C. O., and Arturo M. M.: Diurnal, seasonal and annual variation in the net
e	cosystem CO ₂ exchange of a desert shrub community (Sarcocaulescent) in Baja California,
Ν	Iexico, Global Change Biology, 11, 927-939, 2005.

Sims P.L., Bradford J. A.: Carbon dioxide fluxes in a southern plains prairie. Agricul. For.

- 4 Su, Z., Timmermans, W., Gieske, A., Jia, L., Elbers, J. A., Olioso, A., Timmermans, J., Van Der
- 5 Velde, R., Jin, X., Van Der Kwast, H., Nerry, F., Sabol, D., Sobrino, J. A., Moreno, J. and
- 6 Bianchi, R.: Quantification of land-atmosphere exchanges of water, energy and carbon dioxide in
- 7 space and time over the heterogeneous Barrax site, International Journal of Remote Sensing,
- 8 29:17, 5215- 5235, 2008.
- 9 Suyker A. E., and Verma S. B.: Year-round observations of the net ecosystem exchange of carbon
 10 dioxide in a native tallgrass prairie. Glob. Change Biology, 7, 279-289, 2001.
- 11 Toda M., Nishida K., Ohte, N. Tani M., and Musiake K. : Observations of Energy Fluxes and
- 12 Evapotranspiration over Terrestrial Complex Land Covers in the Tropical Monsoon Environment,
- 13 *Journal of the Meteorological Society of Japan* 80(3), 465-484, 2002.

- Seasonal variations in the net ecosystem CO2 exchange of a mature Amazonian transitional
 tropical forest (cerradão), *Functional Ecology*, 15, 388-395, 2001.
- 17 Webb E. K., Perman G. I., and Leuning R.: Correction of flux measurements for density effects due
- 18 to heat and water transfer. Quart, J. Roy. Meteor. Soc., 106, 85-100, 1980.

¹⁴ Vourlitis G. L., Filho N. P., Hayashi M. M. S., Nogueira J. De. S., Caseiro F. T., and Campelo J. H.:

1	Wever L. A., Flanagan, L. B., and Carlson, P.J.: Seasonal and interannual variation in
2	evapotranspiration, energy balance, and surface conductance in northern temperate grassland.
3	Agricul. For. Meteorol. 112, 31-49, 2002.
4	Wicke W., and Bernhofer C.: Energy balance comparison of the Hartheim Forest and an adjacent
5	grassland site during the HartX Experiment, Theor. Appl. Climatol. 53, 49-58, 1996.
6	Woodward F. L., Lomas M. R., and Betts R. A.: Vegetation-climate feedbacks in a greenhouse world.
7	Philosophical Transactions of the Royal Society, London, 353, 29-39, 1998.
8	Xue Y., Juang H. M., Li W., Prince S., DeFries R, Jiao Y, and Vasic R.: Role of land surface
9	processes in monsoon development: East Asia and West Africa. J. Geophy. Res., 109, D03105,
10	doi:10.1029/2003JD003556, 2004.
11	
12	Figure Captions
12 13	Figure Captions Figure 1. Photo of the setup at the measurement site.
13	Figure 1. Photo of the setup at the measurement site.
13 14	Figure 1. Photo of the setup at the measurement site.Figure 2. Meteorological data collected at the grassland site during the period from June
13 14 15	Figure 1. Photo of the setup at the measurement site.Figure 2. Meteorological data collected at the grassland site during the period from June 2007 to June 2008 at the steppe prairie site.
13 14 15 16	 Figure 1. Photo of the setup at the measurement site. Figure 2. Meteorological data collected at the grassland site during the period from June 2007 to June 2008 at the steppe prairie site. Figure 3 Footprint flux and contributions of the cumulative flux according to Eq. (5) for
13 14 15 16 17	 Figure 1. Photo of the setup at the measurement site. Figure 2. Meteorological data collected at the grassland site during the period from June 2007 to June 2008 at the steppe prairie site. Figure 3 Footprint flux and contributions of the cumulative flux according to Eq. (5) for neutral stability where U = 3.98 m s⁻¹, z = 4.0 m, d = 0.2 m, and u_* = 0.30 m
 13 14 15 16 17 18 	 Figure 1. Photo of the setup at the measurement site. Figure 2. Meteorological data collected at the grassland site during the period from June 2007 to June 2008 at the steppe prairie site. Figure 3 Footprint flux and contributions of the cumulative flux according to Eq. (5) for neutral stability where U = 3.98 m s⁻¹, z = 4.0 m, d = 0.2 m, and u_* = 0.30 m s⁻¹.
 13 14 15 16 17 18 19 	 Figure 1. Photo of the setup at the measurement site. Figure 2. Meteorological data collected at the grassland site during the period from June 2007 to June 2008 at the steppe prairie site. Figure 3 Footprint flux and contributions of the cumulative flux according to Eq. (5) for neutral stability where U = 3.98 m s⁻¹, z = 4.0 m, d = 0.2 m, and u_* = 0.30 m s⁻¹. Figure 4. Seasonal variations of weekly mean downward shortwave radiation (DSR),

1	Figure 5. Seasonal variations of weekly mean net radiation (Rn) , sensible heat flux (H) ,
2	latent heat flux (<i>LE</i>), soil heat flux (G_0) and CO_2 flux (F_{CO_2}) during the period
3	from June 2007 to June 2008 at the steppe prairie site.
4	Figure 6. Diurnal variations of weekly mean downward shortwave radiation (DSR), upward
5	shortwave radiation (USR), downward longwave radiation (DLR), upward longwave
6	radiation (ULR) and surface albedo during the period from June 2007 to June 2008 at
7	the steppe prairie site.
8	Figure 7. Diurnal variation of weekly mean net radiation (Rn) , sensible heat flux (H) ,
9	latent heat flux (<i>LE</i>), soil heat flux (G_0) and CO_2 flux (F_{CO_2}) during the period from
10	June 2007 to June 2008 at the steppe prairie site
11	Figure 8. Inter-comparison of the measured $(H + LE)$ against available energy $(Rn - G_0)$
12	during the period from June 2007 to June 2008 at the steppe prairie site.
13	Figure 9. Temporal variations of soil surface temperature (K) and at the depths of 0.05 m,
14	0.10 m, 0.15 m, 0.2 m, and 0.4 m, and of soil water content at the depths of 0.10 m,
15	0.20 m, and 0.5 m.
16	Figure 10. Diurnal variation of downward shortwave radiation (DSR), upward shortwave
17	radiation (USR), downward longwave radiation (DLR), upward longwave radiation
18	(ULR) and surface albedo on June 7, 2008, and on December 22, 2007 at the steppe
19	prairie site.
20	Figure 11. Diurnal variations of net radiation (Rn) , sensible heat flux (H) , latent heat flux
21	(<i>LE</i>), soil heat flux (G_0), and CO_2 flux (F_{CO_2}) on June 7, 2008 and on December 22,
22	2007 at the steppe prairie site.

- 1 Figure 12. Surface energy partitioning on June 7, 2008 and on December 22, 2007 at the
- 2 steppe prairie site.

3